Fingering Instabilities of Confined Elastic Layers in Tension

Kenneth R. Shull, Cynthia M. Flanigan, and Alfred J. Crosby
Department of Materials Science and Engineering, Northwestern University, 2225 North Campus Drive, Evanston, Illinois 60208-3108
(Received 28 September 1999)

Fingering instabilities similar to those commonly observed in viscous systems have been observed in purely elastic layers that are strained in tension. The instability is driven by the release of lateral constraints within a confined elastic layer and is observed when the lateral confinement significantly exceeds the thickness of the elastic layer. Our results show convincingly that yielding or flow of a material is not required in order for fingering to be initiated in a confined material.

PACS numbers: 46.32.+x, 68.35.Gy, 83.80.Dr

In many applications, an elastic or viscoelastic material is confined between two rigid surfaces and subjected to tensile forces. Extension to large strains requires fibrillation, the onset of which is commonly attributed to flow instabilities arising from the viscous response of the material. The classic Saffman-Taylor instability of a Newtonian fluid is the most famous example of this type of behavior [1]. Similar instabilities are observed in a wide range of situations, including peeling of a pressure sensitive adhesive and crazing in glassy polymers [2]. A common feature in all of these situations is that the magnitude of the negative hydrostatic stress in front of an advancing interface increases in the direction of interfacial motion (the x direction in our notation). In the Saffman-Taylor problem involving flow of a Newtonian liquid, an estimate for λ, the wavelength of the lateral perturbation in the shape of the interface, is determined by a balance between the pressure gradient, $d\sigma/dx$, and the surface energy, γ,

$$\lambda = 2\pi[\gamma/(d\sigma/dx)]^{1/2}. \tag{1}$$

The instability is not limited to Newtonian fluids, but is observed for many non-Newtonian fluids, and for solids as well. For example, in a perfectly plastic material, the relevant stress gradient is determined by the yield stress, τ_0. Equation (1) can still be used in this case, with the stress gradient given by τ_0/h, where h is the thickness of the plastic layer [3]. It is, in fact, generally accepted that the ability of a material to yield or flow in some way is required in order for shape instabilities associated with the onset of fingering to be observed. In this Letter, we show that these shape instabilities are observed in purely elastic materials at suitably high strains, and that the formation of these fingers is not suppressed by elastic restoring forces.

While fingering instabilities in thin layers are generally attributed to some type of flow, the stresses which ultimately lead to viscous fingering may originate from the elastic character of the material [4]. The simplest way to illustrate this point is to consider the stress distribution under a flat cylindrical punch of radius a, which is placed in contact with a linearly elastic layer of thickness h. The shape of the stress distribution within the layer, which we assume to be incompressible, is determined by the lateral confinement, which is in turn characterized by the quantity a/h. For a punch that is adhesively bonded to a thick layer (low a/h) and placed in tension, the normal stress, σ_{zz}, at the surface of the punch has a maximum value at the periphery of the punch ($r = a$) because of the stress concentration there. In the limit of an infinitely thick elastic layer, the tensile normal stress is given by the following expression [5]:

$$\sigma_{zz}(r) = \frac{\sigma_{\text{avg}}}{[1 - (r/a)^2]^{1/2}}, \tag{2}$$

where σ_{avg} is the average tensile stress applied by the punch. For thinner layers, lateral stresses arising from the confinement of the material give a maximum stress at the center of the punch. In the limit of very thin, incompressible layers ($a/h = \infty$) the normal stress is approximately equal to the hydrostatic stress, and is given by the following asymptotic expression [6]:

$$\sigma_{zz}(r) = 2\sigma_{\text{avg}}[1 - (r/a)^2]. \tag{3}$$

In order to illustrate the change in shape of the stress distribution as the degree of confinement varies between the limits corresponding to Eqs. (2) and (3), we have performed finite element calculations for different values of a/h. The confined layer is assumed to be incompressible, with a linearly elastic response. The results of these calculations are shown in Fig. 1. For $a/h = 1$, the normal stress at the surface of the punch decreases monotonically from the edge of the punch ($a/r = 1$) to its center ($a/r = 0$). For larger values of a/h, however, we see that the tensile stress reaches a minimum at a finite value of a/r, and begins to increase toward the center of the punch. In this region the sign of the stress gradient meets the requirement for viscous fingering outlined above. The question that we have addressed experimentally concerns the possibility of "elastic" fingering in a material where flow is suppressed.

In our experiments a thin layer of an elastic material is adhesively bonded to two rigid surfaces, as illustrated schematically in Fig. 2. The elastic material is a physically cross-linked polymer gel made by dissolving an acrylic triblock copolymer in 2-ethyl hexanol. The triblock copolymer has poly(methyl methacrylate) (PMMA) end blocks

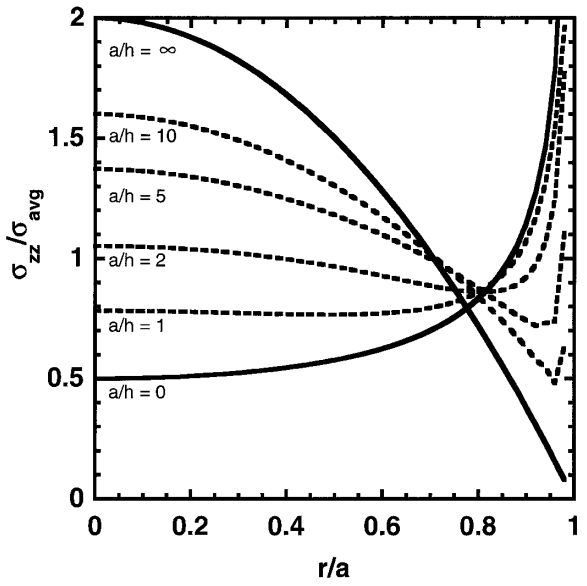

FIG. 1. Normal stress distribution for a flat, cylindrical punch bonded to a thin elastic layer for different values of a/h. The stresses are normalized by the average stress, σ_{avg}, given by $P/\pi a^2$, where P is the applied tensile load.

that are covalently linked to a poly(n-butyl acrylate) midblock. These materials are freely flowing liquids at temperatures above 65 °C. At lower temperatures, the PMMA blocks aggregate to form ideally elastic solids, with no discernible creep behavior over the time scales of our experiments [7,8]. These materials were molded into uniform layers with a uniform thickness, h. The glass slides used as substrates for the gel layers were coated with a styrene-acrylonitrile copolymer that provided good adhesion between the gel and the glass.

Optically smooth, hemispherical glass lenses were used as the second contacting surface. These indenters were coated with a 100 nm layer of PMMA, which was floated onto the lenses to serve as an adhesion promoter between the gel and the lens. Measurements of the load/displacement relationship were made as described previously [9,10]. An inchworm stepping motor placed in a series with a 50 g load transducer was used to control the displacement between the gel layer and the glass indenter. An optical microscope connected to a CCD camera was positioned directly above the sample to record the changes in the contact area during the test. The applied displacement was measured directly by a fiber optic displacement sensor.

In a typical experiment, the lens is brought into contact with the elastic gel, which is then heated to approximately 70 °C. The gel flows somewhat under these conditions, thereby increasing the contact radius, a, between the spherical indenter and the top surface of the gel. The PMMA blocks become embedded in the surface coatings, giving very good adhesion of the gel to both confining surfaces after the gel is cooled to room temperature. Mechanical testing then proceeds by extending the gel in tension, with an applied displacement rate of 2 μm/s.

The qualitative behavior observed during the extension tests is determined largely by a/h. Typical behavior observed for $a/h > 3$ is shown in Fig. 3. Here we plot the average stress ($\sigma_{\text{avg}} = P/\pi a^2$, where P is the applied tensile load) as a function of the nominal strain, ε (displacement divided by layer thickness). The displacement was cycled reversibly to demonstrate the elastic nature of the fingering process. For this test, a PMMA coated indenter with a radius of curvature of 3 mm was heated in contact

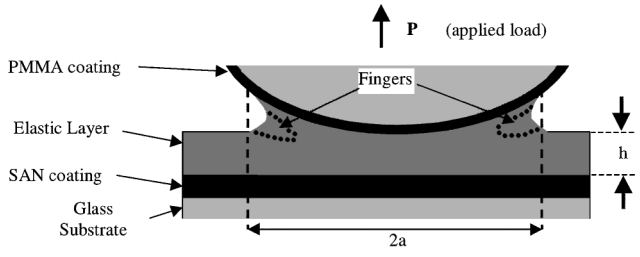

FIG. 2. Schematic of the testing geometry, showing fingers propagating into the elastic layer.

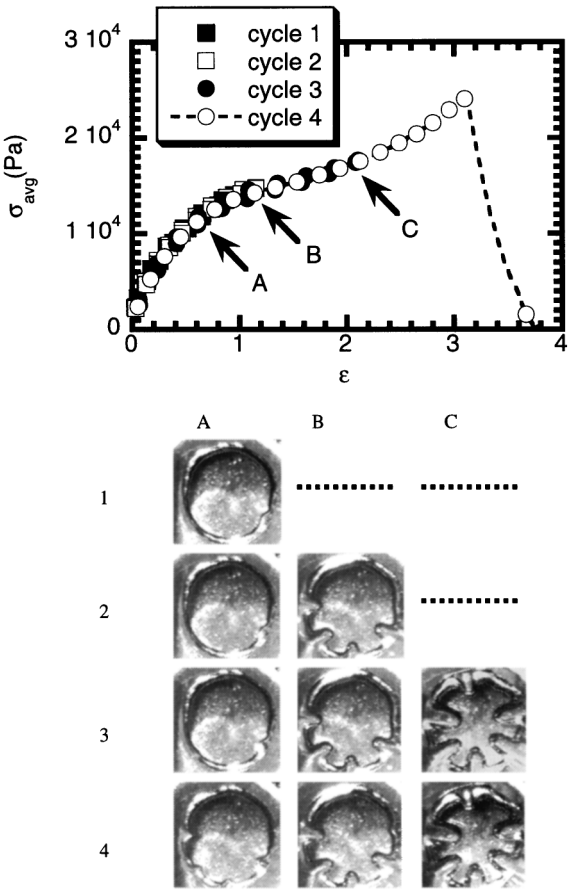

FIG. 3. Stress/strain curve for a confined elastic layer with $a/h = 5.0$ during cyclical tensile loading. The images correspond to the indicated points on the stress/strain curve, taken during the four different cycles as described in the text.

with a 0.25 mm thick gel layer producing a contact area with a radius of 1.3 mm. Because of the curvature of the indenter, the thickness of the sample (corresponding to the spacing between the indenter and the flat, rigid substrates) varies from about 0.25 mm at $r = 0$ to 0.5 mm at $r = a$. Values used to calculate the nominal strain correspond to the original layer thickness, which is close to the minimum thickness of the layer. The modulus, E, of the elastic layer for the experiment corresponding to Fig. 3 is 10^4 Pa, and the images correspond to the indicated points along the stress/strain curve.

The images at point A illustrate the onset of the instability within the gel column, corresponding to a critical value of the nominal strain near 0.72. The gel layer is further extended to a strain of 0.95, where the perturbation to the circular cross section of the gel becomes more prominent. Cycle 1 is completed by compressing the elastic layer into the glass indenter in order to recover a zero load. Cycles 2 and 3 extend to points B ($\varepsilon = 1.15$) and C ($\varepsilon = 2.10$), respectively. Images corresponding to these points are shown as well. Careful inspection of these images reveals that the contact area between the indenter and elastic layer does not change during these cyclic tests. Rather, the shape instabilities correspond to fingers that propagate into the bulk column of the gel as illustrated schematically in Fig. 2. As shown by the comparison of images during each cycle in Fig. 3, the gel recovers its original shape after cycling through various strains. The fourth cycle terminates with cohesive fracture of the gel at $\varepsilon = 3.1$, with a fracture plane midway between the two confining surfaces. The general features of the elastic instability, including the characteristic spacing between fingers, was quite repeatable from sample to sample.

While our discussion of the instabilities that develop in strained samples confined between two rigid plates has focused on elastic layers in contact with a curved, axisymmetric indenter, this behavior is observed with other confined geometries as well. The onset and development of fingering within these elastic gels have been repeated for a wedge test, where a gel is confined between two PMMA coated glass slides separated by 1 mm glass shims. After heating the gel in contact with both surfaces and allowing it to cool to form an elastic solid, a wedge is driven between the rigid plates using a linear stepping motor. While this experiment is more difficult to control in a quantitative and reproducible manner, fingering instabilities at relatively high strains were observed in these situations as well. These measurements indicate that the fingering instabilities commonly observed in peeling experiments do not necessarily require flow of the confined adhesive layer.

From experiments with different values of a and h, we find that the fingering instability is observed only for $a/h > 2.5$. A second observation is that the shape instabilities appear only when a critical strain near 0.5 is exceeded. These features can be explained qualitatively by considering the elastic strain energy in the gel as deformation proceeds. In order to minimize the total energy required to extend a confined layer, fingers develop within the strained material. These instabilities eliminate the lateral constraints within the confined gel layers. Using a simplistic approach, we can show that under certain conditions of strain and confinement, some form of nonuniform deformation becomes energetically favorable.

We begin by assuming a linear relationship between load and displacement, in which case the following expression relates the strain energy, U, to the load, P, the displacement, δ, and the compliance, C ($C \equiv \delta/P$):

$$U = \int P d\,\delta = \frac{1}{C}\,\frac{\delta^2}{2}. \tag{4}$$

The elastic gels that we utilize in our experiments are not linearly elastic at high strains in uniaxial extension, but show a nonlinear response that is consistent with rubber elasticity theory. Nevertheless, the simple linear analysis presented here gives an adequate qualitative description of the confinement effects that lead to the fingering instability. For an incompressible elastic layer, the compliance is given by the following function [10]:

$$C(a,h) = \frac{3}{8Ea}\left\{1 + 1.33\,\frac{a}{h} + 1.33\left(\frac{a}{h}\right)^3\right\}^{-1}. \tag{5}$$

The rapid decrease of the compliance with increasing a/h is responsible for nonuniform deformation, of which fingering is one example. Conceptually, for values of a/h that are larger than approximately 1, it is energetically favorable for one large bonded region to be split into several smaller regions. In our case this occurs by fingering, which alleviates some of the lateral constraints responsible for the decreased compliance.

This purely elastic argument does not account for deviations in the Laplace pressure within the elastic material. These effects are accounted for in the linear stability analysis from which Eq. (1) was derived. An estimate of the critical wavelength of the perturbation can be estimated from Eq. (1) and the stress distributions shown in Fig. 1. This approach amounts to a linear stability analysis that neglects changes in the elastic stress field as the perturbation develops. As stated earlier the requirement for the appearance of a stress-induced instability is that the tensile stress in the material increases towards its interior. For the cylindrical punch geometry this condition is met for $a/h > 1$, as illustrated by the data in Fig. 1. A more detailed analysis of these data shows that, for a/h between 2 and 10, the maximum magnitude of the appropriate stress gradient is approximately equal to $0.25\sigma_{\text{avg}}/h$, and that this maximum gradient occurs at values of a/r that are between 0.6 and 0.85. Using this value for the stress gradient in Eq. (1) gives $\lambda \approx 4\pi(\gamma h/\sigma_{\text{avg}})^{1/2}$. The surface energy of the gels used in our experiments is close to 30 mJ/m^2, which with $h = 0.25$ mm and $\sigma_{\text{avg}} = 10^4$ Pa

gives $\lambda = 0.35$ mm, a figure that is in reasonable agreement with the observed wavelength. This length is, of course, close to the thickness of the elastic layer, which can be viewed as a lower cutoff for λ. We have noticed in several preliminary tests on layers with different thicknesses that the fingering wavelength is generally comparable to the film thickness.

In order for a confined elastic material to be extended to large strains, some mechanism for reducing the lateral confinement must be provided. We have shown that for intermediate confinement levels (a/h between about 2 and 5 in our experiments) this confinement reduction is accomplished by fingering. For a greater degree of confinement, obtained, for example, with very large values of a/h, other mechanisms need to be considered. In these cases it will be more favorable for cavitation to take place in the center of the material than for the fingers to continue to propagate all the way to the center of the contact area. Cavitation requires that bonds within the material be ruptured, or that adhesive failure occur at the interface between the elastic layer and one of the confining surfaces. Cavitation dominates the behavior for very large values of a/h, both for purely elastic solids [11] and for more viscoelastic pressure sensitive adhesives [12,13]. Also, while we have shown that fingering instabilities do occur in purely elastic materials, some flow or yielding will still play a role in many practical situations. For example, yielding may take place once fibrillation has already been initiated. Indeed, extension of the fibrils to the very high strains commonly observed in pressure sensitive adhesives will certainly require that some yielding take place. We have shown in this Letter, however, that the onset of the instability that ultimately leads to fibrillation can be a purely elastic phenomenon.

This work was funded by the NSF (Grant No. DMR-9457923). Acknowledgment is also made to the donors of the Petroleum Research Fund for partial support of this work. The authors have also benefited from many helpful discussions with Dr. H. R. Brown and Dr. C. F. Creton.

[1] P. G. Saffman and G. I. Taylor, Proc. R. Soc. London A **245**, 312 (1958).
[2] A. S. Argon and M. Salama, Mater. Sci. Eng. **23**, 219 (1976).
[3] R. J. Fields and M. F. Ashby, Philos. Mag. **33**, 33 (1976).
[4] S. H. Spiegelberg and G. H. McKinley, J. Non-Newton. Fluid Mech. **67**, 49 (1996).
[5] I. N. Sneddon, Int. J. Eng. Sci. **3**, 47 (1965).
[6] A. N. Gent, Rubber Chem. Technol. **67**, 549 (1994).
[7] C. L. Mowery, A. J. Crosby, D. Ahn, and K. R. Shull, Langmuir **13**, 6101 (1997).
[8] C. M. Flanigan and K. R. Shull, Langmuir **15**, 4966 (1999).
[9] D. Ahn and K. R. Shull, Macromolecules **29**, 4381 (1996).
[10] K. R. Shull, D. Ahn, W.-L. Chen, C. M. Flanigan, and A. J. Crosby, Macromol. Chem. Phys. **199**, 489 (1998).
[11] A. N. Gent and P. B. Lindley, Proc. R. Soc. London A **249**, 195 (1958).
[12] H. Lakrout, P. Sergot, and C. Creton, J. Adhes. **69**, 307 (1999).
[13] C. Gay and L. Leibler, Phys. Rev. Lett. **82**, 936 (1999).